AN ANALYTICAL APPROACH ON THE BUCKLING ANALYSIS OF CIRCULAR, SOLID AND ANNULAR FUNCTIONALLY GRADED THIN PLATES

H. Koohkan[1], A. Kimiaeifar[2]*, A. Mansourabadi[3] and R. Vaghefi[1]
[1]Department of Mechanical Engineering, Shahid Bahonar University, Kerman, Iran.
[2]Department of Mechanical Engineering, Aalborg University, Aalborg, Denmark.
[3]Department of Mechanical Engineering, Persian Gulf University of Bushehr, Bushehr, Iran.
*Corresponding email: a.kimiaeifar@gmail.com.

Abstract: *In this paper, the buckling analysis of circular, solid and annular functionally graded thin plates under uniform radial compression loads is studied. The material properties through the thickness are assumed to be power functions of the thickness. Moreover, the stability equations based on the classical plate theory (CPT), are derived by using the Hamilton's principle. The obtained coupled-PDEs are difficult to be used for evaluation of the buckling loads of annular plates with various boundary conditions. To resolve this difficulty, a coordinate transformation from the middle plane to a new position is done and as consequence the equations are decoupled. By using the forgoing equations, the buckling loads are determined. The procedure is done for both circular and annular FGM plates of various boundary conditions under uniform radial loads on the edges and the results are validated with one of references.*

Key Words: *Buckling analysis; solid plate; annular plate; functionally graded materials.*

INTRODUCTION

Functionally graded materials (FGMs) are a kind of composite materials which include continuously varying mechanical properties. Recently, these materials are widely used in manufacturing for special engineering applications such as nuclear reactors and chemical plants [1-2]. Also, these materials are been widely applied in the aerospace and airplane industries [3]. Vast applications of FGMs make it necessary to consider buckling capacity of these structures. This subject has attracted a lot of researches to study the mechanical and thermal buckling of FGMs. Buckling analysis of solid circular FGM plates is done by Najafizadeh and Eslami [4]. They derived the equilibrium and stability equations of a FGM circular plate under uniform radial compression loads. They considered the classical plate theory and solved coupled stability equations to obtain buckling loads. Other researchers [5-6] studied the thermal and mechanical buckling of rectangular FGM plates using the classical and high order plate theories. An exact solution for the buckling of FGM circular plates under uniform radial compression by using higher order shear deformation plate theory is presented by Najfizadeh and Heydari [7]. Also, Koohkan et al [8] analyzed annular functionally graded thin plates by using an analytical method. Abrate [9,10] studied the free vibration, buckling, and static deflections of FGM plates. He showed that FGM plates behave like homogeneous ones and their behavior can be predicted. In the present paper buckling loads of circular, solid and annular FGM plates under pressure loads are calculated. First, Stability equations are derived through the variational formulation then by using an elegant method without solving coupled equations, buckling loads are calculated. Annular plates with different boundary conditions are considered. The results can also be used for FGM rings which are so applied as structural members in engineering designs.

BRIEF REVIEW OF THE BASIC EQUATIONS FOR FGM CIRCULAR PLATES

Power functions of the thickness circular plate composed of ceramic and metal is considered. The z component of coordinate axes is positioned along the plate thickness. Therefore, the modulus of elasticity E is considered as follows

$$E = E(z) = E_m + (E_c - E_m)(\frac{2z+h}{2h})^k \quad (1)$$

where E_c and E_m are the Young's modulus of the ceramic and metal, respectively. In Eq. (1), h presents the plate thickness while k shows the volume fraction exponent. However, the Poisson's ratio is assumed to be constant. To obtain the total potential energy of the plate, strain energy is added to potential energy of external loads as follows

$$V = U + \Omega \quad (2)$$

where U is the strain energy and can be obtained as follows:

$$U = \frac{1}{2}\int_0^r\int_0^{2\pi}\int_{-h/2}^{h/2}\varepsilon_{ij}\sigma_{ij}\, rdrd\theta dz = \frac{1}{2}\int_0^r\int_0^{2\pi}\int_{-h/2}^{h/2}(\varepsilon_{rr}\sigma_{rr} + \varepsilon_{\theta\theta}\sigma_{\theta\theta} + \varepsilon_{r\theta}\sigma_{r\theta})\, rdrd\theta dz \quad (3)$$

where ε_{ij} and σ_{ij} are the strain and stress components, respectively. By considering a plane-stress condition the two dimensional stress–strain law can be expressed as bellow:

$$\varepsilon_{rr} = \frac{1}{E(z)}(\sigma_{rr} - \nu\sigma_{\theta\theta}) \tag{4}$$

$$\varepsilon_{\theta\theta} = \frac{1}{E(z)}(\sigma_{\theta\theta} - \nu\sigma_{rr}) \tag{5}$$

$$\varepsilon_{r\theta} = \frac{1}{G(z)}\sigma_{r\theta} \tag{6}$$

Applying Love–Kirchhoff assumptions ε_{zr} and $\varepsilon_{z\theta}$ (out of plane shear deformations) are disregarded because the plate is assumed thin. The strain components with the distance z from the middle plane are given by:

$$\varepsilon_{rr} = \bar{\varepsilon}_{rr} + zk_{rr} \tag{7}$$

$$\varepsilon_{\theta\theta} = \bar{\varepsilon}_{\theta\theta} + zk_{\theta\theta} \tag{8}$$

$$\varepsilon_{r\theta} = \bar{\varepsilon}_{r\theta} + 2zk_{r\theta} \tag{9}$$

where $\bar{\varepsilon}_{ij}$ and k_{ij} are the engineering strain components and the curvatures, respectively which can be obtained by

$$\bar{\varepsilon}_{rr} = \frac{\partial u}{\partial r} + \frac{1}{2}(\frac{\partial w}{\partial r})^2 \tag{10}$$

$$\bar{\varepsilon}_{\theta\theta} = \frac{1}{r}\frac{\partial v}{\partial \theta} + \frac{u}{r} + \frac{1}{2}(\frac{1}{r}\frac{\partial w}{\partial \theta})^2 \tag{11}$$

$$\bar{\varepsilon}_{r\theta} = \frac{1}{r}\frac{\partial u}{\partial \theta} + \frac{\partial v}{\partial r} - \frac{v}{r} + (\frac{1}{r}\frac{\partial w}{\partial \theta})\frac{\partial w}{\partial \theta} \tag{12}$$

and

$$k_{rr} = -\frac{\partial^2 y}{\partial r^2} \tag{13}$$

$$k_{\theta\theta} = -\frac{1}{r}\frac{\partial w}{\partial r} - \frac{1}{r^2}\frac{\partial^2 w}{\partial \theta^2} \tag{14}$$

$$k_{r\theta} = -\frac{1}{r}(\frac{\partial^2 w}{\partial r \partial \theta}) + \frac{1}{2r^2}\frac{\partial w}{\partial \theta} \tag{15}$$

where u, v and w represent the corresponding components of the displacement of a point on the mid-plate surface. In Eq. (2), Ω , the potential energy of external loads is given by

$$\Omega = -\int_0^r \int_0^{2\pi} p_r urdrd\theta \tag{16}$$

where pr is the r component of the external load over surface of the plate element. By substitution Eqs. (4-9) into Eq. (3), integrating with respect to z from $-\frac{h}{2}$ to $\frac{h}{2}$, and adding Eq. (16), the total potential energy is obtained as follows:

$$V = \int\int Fr\, dr\, d\theta \tag{17}$$

where

$$\begin{aligned} F = {} & \frac{A}{2(1-\nu^2)}[\bar{\varepsilon}_{rr}{}^2 + \bar{\varepsilon}_{\theta\theta}{}^2 + 2\nu\bar{\varepsilon}_{rr}\bar{\varepsilon}_{\theta\theta} + \frac{1-\nu}{2}\bar{\varepsilon}_{r\theta}{}^2] \\ & + \frac{B}{(1-\nu^2)}[\bar{\varepsilon}_{rr}\, k_{rr} + \bar{\varepsilon}_{\theta\theta}\, k_{\theta\theta} + \\ & \nu(\bar{\varepsilon}_{rr}k_{\theta\theta} + \bar{\varepsilon}_{\theta\theta}k_{rr}) + (1-\nu)\bar{\varepsilon}_{r\theta}k_{r\theta}] + \\ & \frac{C}{2(1-\nu^2)}[k_{rr}{}^2 + k_{\theta\theta}{}^2 + 2\nu k_{rr}k_{\theta\theta} + 2(1-\nu)k_{r\theta}{}^2] \\ & - P_r \end{aligned} \tag{18}$$

where

$$A = \int_{-h/2}^{h/2} E(z)\, dz, \tag{19}$$

$$B = \int_{-h/2}^{h/2} E(z)\, zdz, \tag{20}$$

$$C = \int_{-h/2}^{h/2} E(z)\, z^2 dz, \tag{21}$$

Eq. (1) is considered to define the forgoing parameters as follows:

$$A = h\left(E_m + \frac{E_c - E_m}{k+1}\right), \tag{22}$$

$$B = \frac{kh^2(E_c - E_m)}{2(k+1)(k+2)}, \tag{23}$$

$$C = \frac{h^3}{12}\left\{E_m + \frac{3(k^2+k+2)(E_c - E_m)}{(k+1)(k+2)(k+3)}\right\} \tag{24}$$

By assuming that the plate is subjected to the uniform compression load alone, the total potential energy is a function of the displacement components and their derivatives and might be written as bellow:

$$\begin{aligned} V = \int\int & F(u, v, w, u_{,r}, u_{,\theta}, v_{,r}, v_{,\theta}, w_{,r}, w_{,\theta}, \ldots \\ & w_{,rr}, w_{,r\theta}, w_{,\theta\theta})\, rdrd\theta \end{aligned} \tag{25}$$

STABILITY EQUATIONS

Generally, to derive the stability equations by using energy method, the condition of second variation of the total potential energy is used, Brush and Almorth [11]. To determine the second variation condition, the following rule, namely Trefftz rule ($\bar{\delta}(\delta^2 V) = 0$), is considered. This rule provides the governing equations that determine the buckling load. To achieve this goal the displacement components are defined as follows:

$$u = u_0 + u_1 \tag{26}$$

$$v = v_0 + v_1 \tag{27}$$

$$w = w_0 + w_1 \tag{28}$$

where, u_0, v_0, w_0 present the primary state of equilibrium and u_1, v_1, w_1 show arbitrary small increments of displacements. Eqs. (10-12,13-15) are substituted into Eq. (18), in order to obtain the total potential energy in terms of displacement components. Treffts rule is applied and the second order terms are collected to obtain following equation.

$$\frac{1}{2}\delta^2 V=\frac{A}{2(1-\nu^2)}\iint\Bigg\{\left(\frac{\partial u_1}{\partial r}\right)^2+\frac{\partial u_0}{\partial r}\left(\frac{\partial w_1}{\partial r}\right)^2+\frac{1}{r^2}\left(\frac{\partial v_1}{\partial\theta}\right)^2+\frac{u_1^2}{r^2}+\frac{1}{r^3}\frac{\partial v_0}{\partial\theta}\left(\frac{\partial w_1}{\partial\theta}\right)^2+\frac{u_0}{r^3}\left(\frac{\partial w_1}{\partial\theta}\right)^2+2\frac{u_1}{r^2}\frac{\partial v_1}{\partial\theta}+2\nu\left(\frac{1}{r}\frac{\partial v_1}{\partial\theta}\frac{\partial u_1}{\partial r}+\frac{u_1}{r}\frac{\partial u_1}{\partial r}\right)+\frac{1}{2r^2}\frac{\partial u_0}{\partial r}\left(\frac{\partial w_1}{\partial\theta}\right)^2+\frac{1}{2r}\frac{\partial v_0}{\partial\theta}\left(\frac{\partial w_1}{\partial r}\right)^2+\frac{u_0}{2r}\left(\frac{\partial w_1}{\partial r}\right)^2+\frac{(1-\nu)}{2}[\frac{1}{r^2}\left(\frac{\partial u_1}{\partial\theta}\right)^2+\left(\frac{\partial v_1}{\partial r}\right)^2+\frac{v_1^2}{r^2}+\frac{2}{r}\frac{\partial u_1}{\partial\theta}\frac{\partial v_1}{\partial r}-\frac{2v_1}{r^2}\frac{\partial u_1}{\partial\theta}+\frac{2}{r^3}\frac{\partial u_0}{\partial\theta}\frac{\partial w_1}{\partial r}\frac{\partial w_1}{\partial\theta}-\frac{2v_1}{r}\frac{\partial u_1}{\partial r}+\frac{2}{r}\frac{\partial v_0}{\partial r}\frac{\partial w_1}{\partial r}\frac{\partial w_1}{\partial\theta}-\frac{2v_0}{r^2}\frac{\partial w_1}{\partial r}\frac{\partial w_1}{\partial\theta}]\Bigg\}r\,dr\,d\theta$$
$$+\frac{B}{1-\nu^2}\iint\Bigg\{-\frac{\partial u_1}{\partial r}\frac{\partial^2 w_1}{\partial r^2}-\frac{1}{r^2}\frac{\partial v_1}{\partial\theta}\frac{\partial w_1}{\partial r}-\frac{u_1}{r^2}\frac{\partial w_1}{\partial r}-\frac{1}{r^3}\frac{\partial v_1}{\partial\theta}\frac{\partial^2 w_1}{\partial\theta^2}-\frac{u_1}{r^3}\frac{\partial^2 w_1}{\partial\theta^2}+\nu\left(-\frac{1}{r}\frac{\partial u_1}{\partial r}\frac{\partial w_1}{\partial r}-\frac{1}{r^2}\frac{\partial^2 w_1}{\partial\theta^2}\frac{\partial u_1}{\partial r}-\frac{1}{r}\frac{\partial v_1}{\partial\theta}\frac{\partial^2 w_1}{\partial r^2}-\frac{u_1}{r}\frac{\partial^2 w_1}{\partial r^2}\right)+(1-\nu)[-\frac{1}{r^2}\frac{\partial^2 w_1}{\partial r\partial\theta}\frac{\partial u_1}{\partial\theta}-\frac{1}{r}\frac{\partial^2 w_1}{\partial r\partial\theta}\frac{\partial v_1}{\partial r}+\frac{v_1}{r^2}\frac{\partial^2 w_1}{\partial r\partial\theta}+\frac{1}{r^3}\frac{\partial w_1}{\partial\theta}\frac{\partial u_1}{\partial\theta}+\frac{1}{r^2}\frac{\partial w_1}{\partial\theta}\frac{\partial v_1}{\partial r}-\frac{v_1}{r^3}\frac{\partial w_1}{\partial\theta}]$$
$$+\frac{C}{2(1-\nu^2)}\iint\Bigg\{\left(\frac{\partial w_1}{\partial r}\right)^2+\frac{1}{r^2}\left(\frac{\partial w_1}{\partial r}\right)^2+\frac{1}{r^4}\left(\frac{\partial^2 w_1}{\partial\theta^2}\right)^2-\frac{2}{r^3}\frac{\partial w_1}{\partial r}\frac{\partial^2 w_1}{\partial\theta^2}+\frac{u_0}{r^3}\left(\frac{\partial w_1}{\partial\theta}\right)^2+2\nu\left(\frac{1}{r}\frac{\partial w_1}{\partial r}\frac{\partial^2 w_1}{\partial r^2}+\frac{1}{r^2}\frac{\partial^2 w_1}{\partial\theta^2}\frac{\partial^2 w_1}{\partial r^2}\right)+2(1-\nu)[\left(\frac{\partial w_1}{\partial\theta}\right)^2+\frac{1}{r^2}\left(\frac{\partial^2 w_1}{\partial r\partial\theta}\right)^2-\frac{2}{r^3}\frac{\partial w_1}{\partial\theta}\frac{\partial^2 w_1}{\partial r\partial\theta}]\Bigg\}r\,dr\,d\theta \tag{29}$$

The Euler equations are applied to the variation in order to derive the stability equations as follows:

$$N_{r1,r}+\frac{1}{r}N_{r\theta 1,\theta}+\frac{N_{r1}-N_{r\theta 1}}{r}=0 \tag{30}$$

$$N_{r\theta 1,r}+\frac{1}{r}N_{\theta 1,\theta}+\frac{2}{r}N_{r\theta 1}=0 \tag{31}$$

$$\frac{C}{1-\nu^2}\nabla^4 w_1-N_{r0}\frac{\partial^2 w_1}{\partial r^2}-\frac{1}{r}N_{\theta 0}\left(\frac{\partial w_1}{\partial r}+\frac{1}{r}\frac{\partial^2 w_1}{\partial\theta^2}\right)-2N_{r\theta 0}\left(-\frac{1}{r^2}\frac{\partial w_1}{\partial\theta}+\frac{1}{r}\frac{\partial^2 w_1}{\partial r\partial\theta}\right)+\frac{B}{1-\nu^2}\left[\frac{1-2\nu}{r^3}\frac{\partial v_1}{\partial\theta}-\frac{1-2\nu}{r^2}\frac{\partial^2 v_1}{\partial r\partial\theta}+\ldots\frac{1}{r^2}\frac{\partial u_1}{\partial r}-\frac{u_1}{r^3}-\frac{2}{r}\frac{\partial^2 u_1}{\partial r^2}-\frac{1}{r^3}\frac{\partial^2 u_1}{\partial\theta^2}\right]-\frac{1}{r^2}\frac{\partial^3 u_1}{\partial\theta^2\partial r}-\frac{1}{r}\frac{\partial^3 v_1}{\partial r^2\partial\theta}-\frac{1}{r3}\frac{\partial^3 v_1}{\partial\theta^3}-\frac{\partial^3 u_1}{\partial r^3} \tag{32}$$

where

$$N_{r1}=\frac{A}{1-\nu^2}\left[\frac{\partial u_1}{\partial r}+\nu\left(\frac{1}{r}\frac{\partial v_1}{\partial\theta}+\frac{u_1}{r}\right)\right]+\frac{B}{1-\nu^2}\left[-\frac{\partial^2 w_1}{\partial r^2}-\frac{\nu}{r}\frac{\partial w_1}{\partial r}-\frac{\nu}{r^2}\frac{\partial^2 w_1}{\partial\theta^2}\right] \tag{33}$$

$$N_{\theta 1}=\frac{A}{1-\nu^2}\left[\frac{u_1}{r}+\frac{1}{r}\frac{\partial v_1}{\partial\theta}+\nu\frac{\partial u_1}{\partial r}\right]+\frac{B}{1-\nu^2}\left[-\frac{1}{r}\frac{\partial w_1}{\partial r}-\frac{1}{r^2}\frac{\partial^2 w_1}{\partial\theta^2}-\nu\frac{\partial^2 w_1}{\partial r^2}\right] \tag{34}$$

$$N_{r\theta 1}=A\left[\frac{1}{r}\frac{\partial u_1}{\partial\theta}+\frac{\partial v_1}{\partial r}-\frac{v_1}{r}\right]+B\left[-\frac{1}{r}\frac{\partial^2 w_1}{\partial r\partial\theta}+\frac{1}{r^2}\frac{\partial w_1}{\partial\theta}\right] \tag{35}$$

$$N_{r0}=\frac{A}{1-\nu^2}\left[\frac{\partial u_0}{\partial r}+\nu\left(\frac{1}{r}\frac{\partial v_0}{\partial\theta}+\frac{u_0}{r}\right)\right]+\frac{B}{1-\nu^2}\left[-\frac{\partial^2 w_0}{\partial r^2}-\frac{\nu}{r}\frac{\partial w_0}{\partial r}-\frac{\nu}{r^2}\frac{\partial^2 w_0}{\partial\theta^2}\right] \tag{36}$$

$$N_{\theta 0}=\frac{A}{1-\nu^2}\left[\frac{u_0}{r}+\frac{1}{r}\frac{\partial v_0}{\partial\theta}+\nu\frac{\partial u_0}{\partial r}\right]+\frac{B}{1-\nu^2}\left[-\frac{1}{r}\frac{\partial w_0}{\partial r}-\frac{1}{r^2}\frac{\partial^2 w_0}{\partial\theta^2}-\nu\frac{\partial^2 w_0}{\partial r^2}\right] \tag{37}$$

$$N_{r\theta 0} = A\left[\frac{1}{r}\frac{\partial u_0}{\partial \theta} + \frac{\partial v_0}{\partial r} - \frac{v_0}{r}\right] + B\left[-\frac{1}{r}\frac{\partial^2 w_0}{\partial r \partial \theta} + \frac{1}{r^2}\frac{\partial w_0}{\partial \theta}\right] \quad (38)$$

An axisymmetric buckling of a circular plate subjected to the uniform compressive load −P along its edge is considered. Therefore, $\beta_\theta = P_\theta = P_z = 0$ and with this condition, the stability equations are rewritten as follows

$$\frac{A}{1-\nu^2}\left(\frac{d^2 u_1}{d^2 r^2} + \frac{1}{r}\frac{du_1}{dr} - \frac{u_1}{r^2}\right) + \frac{B}{1-\nu^2}\left(-\frac{d^3 w_1}{dr^3} - \frac{1}{r}\frac{d^2 w_1}{dr^2} + \frac{1}{r^2}\frac{dw_1}{dr}\right) = 0 \quad (39)$$

$$\frac{C}{1-\nu^2}\nabla^4 w_1 - N_{r0}\frac{d^2 w_1}{dr^2} - \frac{1}{r}N_{\theta 0}\frac{dw_1}{dr} + \frac{B}{1-\nu^2}\left(\frac{1}{r^2}\frac{du_1}{dr} - \frac{u_1}{r^3} - \frac{2}{r}\frac{d^2 u_1}{dr^2} + \frac{d^3 u_1}{dr^3}\right) = 0 \quad (40)$$

where N_{r0} and $N_{\theta 0}$ are the pre-buckling forces which are equaled to $-P$ while pre-buckling rotations are neglected. The equations (39), (40) are two coupled ordinary differential equations. Considering these equations, buckling loads for plates with different boundary conditions cannot be obtained easily. Herein, a new coordinate system is assumed which is at the distance δ from the previous one [10, 11].

$$z = \bar{z} + \delta \quad (41)$$

where δ is the vertical distance between the forgoing coordinate systems and the new one. The new coordinate is applied and it can be written as follows:

$$\bar{B} = \int_{z_B}^{z_T} E(\bar{z} + \delta)\, \bar{z} d\bar{z} = \int_{-h/2}^{h/2} E(z)(z - \delta) dz = \int_{-h/2}^{h/2} E(z)\, z dz - \delta \int_{-h/2}^{h/2} E(z)\, dz = B - \delta A \quad (42)$$

Now, it is considered $\delta = B/A$ in order to achieve $\bar{B} = 0$. As the vertical displacement in the new coordinate is the same with the previous one, equations (39) and (40) in the new coordinate can be converted to:

$$\frac{\bar{C}}{1-\nu^2}\nabla^4 w_1 - N_{r0}\frac{d^2 w_1}{dr^2} - \frac{1}{r}N_{\theta 0}\frac{dw_1}{dr} = 0 \quad (43)$$

where

$$\bar{C} = \int_{z_B}^{z_T} E(\bar{z} + \delta)\bar{z}^2 d\bar{z} = C - \frac{B^2}{A} \quad (44)$$

Eq. (43) can be rewritten in the following form:

$$\frac{d^4 w}{dr^4} + \frac{2}{r}\frac{d^3 w}{dr^3} - \frac{1}{r^2}\frac{d^2 w}{dr^2} + \frac{1}{r^3}\frac{dw}{dr} + \mu^2\left[\frac{d^2 w}{dr^2} + \frac{1}{r}\frac{dw}{dr}\right] = 0 \quad (45)$$

where

$$\mu^2 = P_r / \bar{C} / 1 - \nu^2 \quad (46)$$

The 4th order Bessel equation is solved to obtain:

$$w(r) = C_1 + C_2 \ln(r) + C_3 J_0(\mu r) + C_4 Y_0(\mu r), \quad (47)$$

where $C_i\,(i = 1,\ldots,4)$ are constants of integration while J_0 and Y_0 are the Bessel functions of the first and second kind of zero orders, respectively.

DEFINING THE PROBLEM DOMAIN AND BOUNDARY CONDITIONS

The problems contain circular, solid and annular thin plates under compression loads. The circular solid plate is considered to be compressed on the edge. It is assumed that the plate has either the clamped or simply supported boundary conditions. Also the annular plate is assumed to be compressed on the both inner and outer edges. The buckling load is calculated for either clamed or simply supported boundary conditions.

Solid circular plate with clamped boundary condition

A circular plate with radius R and clamped boundary condition under pressure load is considered, see Fig. 1.

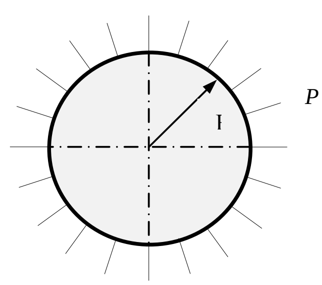

Fig. 1. Solid circle plate under pressure load

Since $w(r)$ must be finite for all values of r, the two terms $\ln(r)$ and $Y_0(\mu r)$ are dropped for the solid plate because they approach an infinity when $r \to 0$. Thus, for the circular plate, Eq. (47) is rewritten as follows

$$w(r) = C_1 + C_3 J_0(\mu r) \quad (48)$$

The edge boundary condition for this plate is given by

$$w(r) = 0\big|_{r=R}, \frac{dw(r)}{dr} = 0\big|_{r=R} \quad (49)$$

The forgoing boundary conditions are substituted into Eq. (48) to obtain the following system of linear homogeneous equations

$$C_1 + C_3 J_0(\mu r) = 0, \quad -\mu C_3 J_1(\mu r) = 0 \tag{50}$$

A nontrivial solution of these equations is found as follows

$$P_{r,cr} = (3.8317)^2 \frac{D}{R^2} = 14.68 \frac{D}{R^2} \tag{51}$$

where

$$D = \frac{\overline{C}}{1-\nu^2} = (C - B^2 / A)/(1-\nu^2) \tag{52}$$

It should be noted that tables of the Bessel functions [12] are used to find the solution.

Solid circular plate with simply supported boundary condition

A circular plate with radius R and simply supported boundary condition under pressure load is considered. The Poisson's ratio is assumed to be 0.3 and the edge boundary conditions are considered as follows:

$$w(r) = 0\Big|_{r=R}, M_r(r) = 0\Big|_{r=R} \tag{53}$$

where

$$M_r = -\overline{C}\left(\frac{d^2 w}{dr^2} + \frac{\nu}{r}\frac{dw}{dr}\right) \tag{54}$$

Substituting the Eq. (48) into the boundary conditions (53) we arrive at the following system of linear homogeneous equations

$$C_1 + C_3 J_0(\mu R) = 0 \tag{55}$$

$$-\overline{C}\mu^2 C_3[\mu R J_0(\mu R) - (1-\nu)J_1(\mu R)] = 0 \tag{56}$$

A nontrivial solution of this system of equations leads to the following

$$\mu r\, J_0(\mu R) - (1-\nu)\, J_1(\mu R) = 0 \tag{57}$$

Letting $\nu = 0.3$ and using the tables of the Bessel function, we can determine the smallest nonzero root of Eq. (57) as

$$(\mu R)_{\min} = 2.0458 \tag{58}$$

where the buckling load can be obtained as follows

$$P_{r,cr} = 4.196 \frac{D}{R^2} \tag{59}$$

Annular plate with inner and outer edges clamped

An annular plate with inner radius $R_i = a$ and outer radius $R_o = b$ under pressure loads on the both edges is considered, see Fig. 2. Eq. (47) is applied while considering the following boundary conditions

$$w(r) = 0\big|_{r=a}, \ \frac{dw(r)}{dr} = 0\Big|_{r=a}, w(r) = 0\big|_{r=b}, \ \frac{dw(r)}{dr} = 0\Big|_{r=b} \tag{60}$$

The answer is yielded to the following system of linear homogeneous equations

$$C_1 + C_2 \ln(r) + C_3 J_0(\mu r) + C_4 Y_0(\mu r) = 0, r = a, b \tag{61}$$

$$C_2 / r - C_3 J_1(\mu r)\mu + C_4 Y_1(\mu r)\mu = 0, r = a, b \tag{62}$$

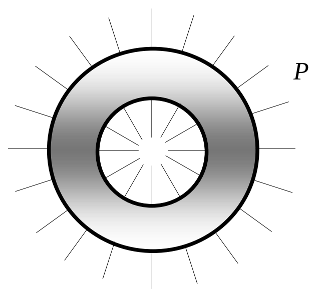

Fig. 2. Annular plate with compressive load on the both inner and outer edges

A nontrivial solution of this system of equations is led to

$$\begin{vmatrix} 1 & \ln(a) & J_0(\mu a) & Y_0(\mu a) \\ 0 & 1/a & -J_1(\mu a)\mu & -Y_1(\mu a)\mu \\ 1 & \ln(b) & J_0(\mu b) & Y_0(\mu b) \\ 0 & 1/b & -J_1(\mu b)\mu & -Y_1(\mu b)\mu \end{vmatrix} = 0, |x| = \det(x) \tag{63}$$

To solve Eq. (63) for determined a and b we can use the tables of the Bessel function, it would determine the smallest μ which leads to the smallest buckling load with respect to $P_{r,cr} = D\mu^2$.

However, it takes time to use the tables of the Bessel function. To solve this problem, Figure (3) is prepared to calculate the buckling load. This figure is plotted using the Bessel function tables. Considering this figure and the following equation the buckling load is calculated more easily.

$$P_{r,cr} = \frac{D\mu'^2}{a^2} \tag{64}$$

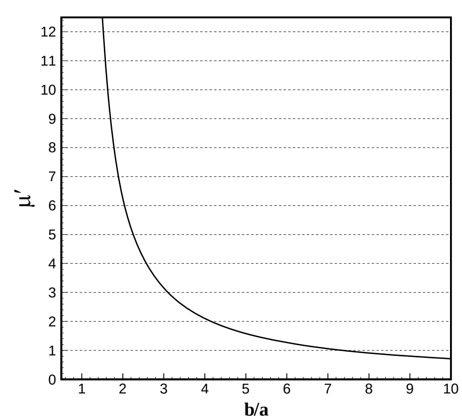

Figure 3: $\mu' = \mu / a$ vs. b/a for an annular plate with inner and outer edges clamped

Annular plate with inner edge simply supported and outer edge clamped

An annular plate with inner edge simply supported and outer edge clamped is considered. The stability equation is solved for this kind of annular plate while the corresponding boundary conditions are considered. Like the previous part to prevent burdensome procedure of using the Bessel function tables; Figure (4) is prepared. Considering this figure and Eq. (64) the buckling load is calculated.

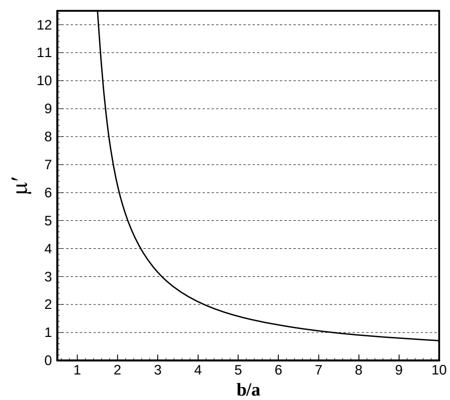

Figure 4: μ' vs.b/a for an annular plate with inner edge simply-supported and outer edge clamped

Annular plate with inner edge clamped and outer edge simply supported or with inner and outer edges simply supported

The buckling loads for these plates are calculated using Eq. (64) and Figures (5, 6) respectively.

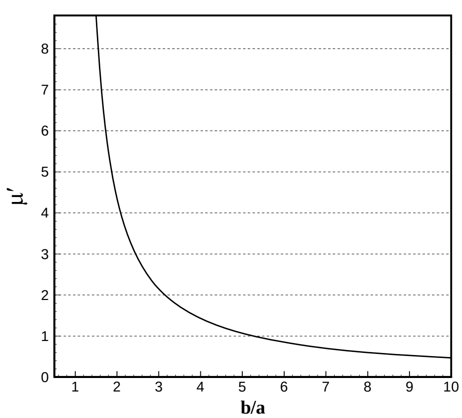

Figure 5: μ' vs. b/a for an Annular plate with inner edge clamped and outer edge simply supported

NUMERICAL RESULTS AND DISCUSSION

As it was discussed, the buckling load for the FGM circular solid and annular plate is obtained without solving coupled stability equations. For the solid circular plate the closed form is obtained while for the annular plates the Bessel function tables are applied to obtain the buckling loads. Considering the closed form solution obtained for the solid circular plate, figures (7, 8) are plotted. The figures show the buckling load versus thickness on radius (h/a) of a circular FGM plate under uniform radial compression with clamped and simply supported boundary conditions, respectively. The combination of materials consists of aluminum ($E_m 70 GPa$, $\nu_m = 0.3$) and alumina ($E_c 380 GPa$, $\nu_c = 0.3$).

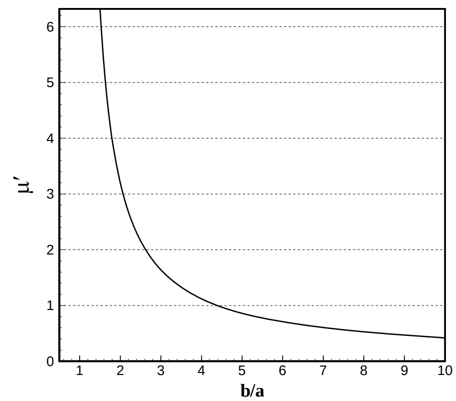

Figure 6: μ' vs. b/a for an Annular plate with inner and outer edges simply supported

It can be seen that the buckling load increases with an increase of (h/a) and decreases with an increase of the volume fraction ratio.

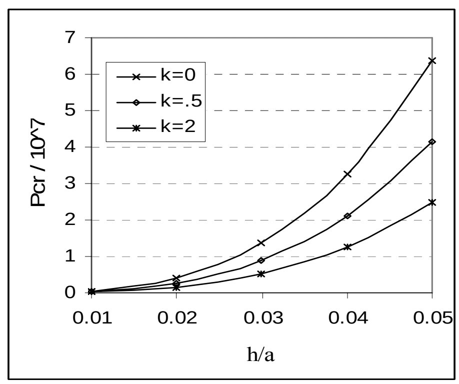

Figure 7: Buckling load vs. thickness on radius of the clamped plate with various volume fraction

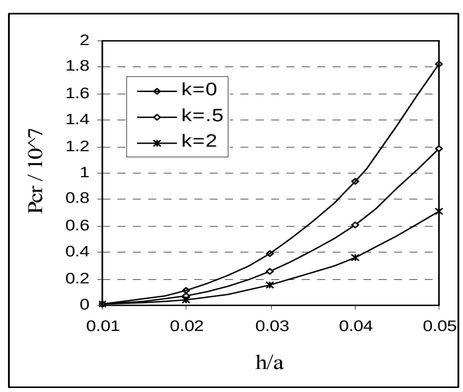

Figure 8: Buckling load vs. thickness on radius of

simply-supported plate; various volume fraction

Evaluating the results obtained for the annular plates, Table 1 is prepared. Homogenous annular plates with different outer to inner radiuses are considered and the results are compared with Yamaki [13]. To obtain the buckling load of a C-C annular plate, Fig. (3) is considered and the result is compared with the reference while a good agreement is seen. The procedure is continued and the buckling load for a S-C annular plate is calculated (using Figure 4) which is normally less than the buckling load of the C-C annular plate with the same geometry. In the same procedure buckling loads for plates with C-S and S-S boundary conditions are calculated (using Figures 5 and 6, respectively) and compared with the reference. It can be seen that the results of Table 1 are a good verification of the presented approach. Table 2 is also prepared in the same procedure while considering the FGM annular plate. Different aspect ratios and volume fraction ratios are considered to show the effect of the variation of the material properties on the buckling load. It should be noted that FGMs composed of aluminum and alumina with the forgoing properties used for plotting Figures 7, 8 are considered. It can be seen that buckling load decreases by increasing the volume fraction ratio.

Table 1: Buckling load for an annular plate; D=1 (C stands for clamp and S for simply support)

P_{cr}	*C-C*		*S-C*		*C-S*		*S-S*	
b/a	present	[Yamaki] (1958)	present	[Yamaki]	present	[Yamaki]	present	[Yamaki]
2	37.06	36.90	22.09	22.18	19.00	19.05	10.24	10.24
10	0.50	0.45	0.39	0.36	0.22	0.22	0.18	0.18

CONCLUSION

Circular, solid or annular plates are widely applied in engineering structures. In the present study, stability equations for FGM circular plates under uniform radial compression loads with the assumption of power law composition for the constituent materials are derived. Also, an analytical solution for the problem is obtained. Moreover, an elegant method is introduced without solving coupled equations arising buckling loads of the circular and annular FGM plates. The results are in very good agreement with those obtained by other references. This study can be used as an accurate reference for many problems in functionally graded materials also for FGM rings which are applied as structural members in engineering designs.

Table 2: Buckling load for an annular FGM plate with different volume fraction (h/a=0.01)

$P_{cr}/10$^5	*C-C*		*S-C*		*C-S*		*S-S*	
b/a	K=0.5	K=2	K=0.5	K=2	K=0.5	K=2	K=0.5	K=2
2	8.360	5.016	4.983	3.990	4.286	2.572	2.310	1.386
10	0.112	0.068	0.088	0.053	0.050	0.028	0.041	0.024

REFERENCES

[1] Yamanouchi M, Koizumi M, Shiota I, 1990, Proceedings of the first international symposium on functionally gradient materials, Sendai, Japan.

[2] Y. Miyamoto, W.A. Kaysser, B.H. Rabin, A. Kawasaki, R.G. Ford, 1999, "Functionally Graded Materials: Design, Processing and Applications", Chapman & Hall, London.

[3] Kimiaeifar, A. and Saidai. A.R., 2008, "Analytical solution for stress analysis in hollow cylinder made of functionally grade materials", Proceeding of the 16th Sc. Conf. Mech. Eng. 13-15 May 2008, Kerman, Iran (ISME 2008).

[4] Najafizadeh MM, Eslami MR, 2002, "Buckling analysis of circular plates of functionally graded materials under uniform radial compression", International Journal of Mechanical Sciences Vol. 4(12), pp. 2479–93.

[5] Javaheri, R and Eslami, M.R., 2002, "Thermal buckling of functionally graded plates based on higher order theory", Journal of Thermal Stresses", Vol. 25(7), pp. 603–25.

[6] Javaheri, R and Eslami, M.R., 2005, "Buckling of functionally graded under inplane compressive loading based on various theories", Iranian Journal of Mechanical Engineering, Vol. 6(1), pp. 76–93.

[7] Najafizadeh, M.M and Heydari, H.R., 2007, "An exact solution for buckling of functionally graded circular plates based on higher order shear deformation plate theory under uniform radial compression", International Journal of Mechanical Sciences, Vol. 50, pp. 603-612.

[8] H. Koohkan, A. R. Saidi, R. Vaghefi, "Analytical solution of annular functionally graded thin plates",

1st International Conference on Composites: characterization, Fabrication, and Application (CCFA1), 2008.

[9] Serge Abrate. 2006. "Free vibration, buckling and static deflections of functionally graded plates", Composites Science and Technology; 66:2383-94.

[10] Serge Abrate, 2008. "Functionally graded plates behave like homogeneous plates", Composites part B: engineering, Vol. 39, pp. 151-8.

[11] Brush DO, Almorth BO. 1975. Buckling of bars, plates and shells. New York: McGraw-Hill, ISBN: 0904 188965

[12] Watson, G.N., 1994. Theory of Bessel functions, 2nd edition, Cambridge University Press, Cambridge. ISBN: 0-521-48391-3

[13] Yamaki N, 1958, "Buckling of a thin annular plate under uniform compression", Transactions of ASME Journal of Applied Mechanics, Vol. 25, pp. 267–73.